

# Novel Design of an Extremely Miniaturized Accelerometer Based on Quantum Tunneling Effect <sup>†</sup>

Michael Haub <sup>\*</sup>, Sebastian Hummel, Martin Bogner and Hermann Sandmaier

Chair Microsystems, University of Stuttgart, Pfaffenwaldring 4F, 70569 Stuttgart, Germany; sebastian.hummel@mst.uni-stuttgart.de (S.H.); martin.bogner@mst.uni-stuttgart.de (M.B.); hermann.sandmaier@mst.uni-stuttgart.de (H.S.)

<sup>\*</sup> Correspondence: michael.haub@mst.uni-stuttgart.de; Tel.: +49-711-685-61820

<sup>†</sup> Presented at the Eurosensors 2018 Conference, Graz, Austria, 9–12 September 2018.

Published: 26 November 2018

**Abstract:** This paper presents the design of an extremely miniaturized accelerometer based on the tunneling effect. Because of its high sensitivity the tunneling effect allows the detection of smallest deflections. The aim of the novel design is a large geometric miniaturization at the lowest possible natural frequency with a nominal acceleration of  $\pm 1$  g corresponding to a deflection of  $\pm 9.36$  Å. The poly-silicon (PolySi) sensor structure with a size ( $L \times W$ ) of  $98 \mu\text{m} \times 85 \mu\text{m}$  is designed in a way that the main displacement operates just in one direction. To lead the sensor into operational conditions, control a constant distance between the tunneling electrodes and perform self-test actuations two electrodes are placed below the sensor structure. The tunneling tip is deposited by a focused ion beam (FIB) to provide the tunneling section with a third pad on the substrate. Within this paper the focus is on the functional implementation of the structure, the investigation of the electrostatic actuators and the deposition of the tunneling tip by the FIB.

**Keywords:** accelerometer; tunneling effect; microsensors; electrostatic; focused ion beam

## 1. Introduction

The necessity of cost reduction in microsensors leads to a constant reduction of their geometric size. Most accelerometers are based on the capacitive principle and consist of a spring-mass-damping-system by deflecting the mass due to an acceleration. The size of these accelerometers amount to several  $100 \mu\text{m} \times 100 \mu\text{m}$ . It is known that the deflection of the mass and the sensitivity of a capacitive sensor decrease quadratically with an isometric reduction of the spring-mass-system. Consequently, smaller and smaller capacities have to be detected. Therefore, the principle of capacitive, piezoresistive or piezoelectric detection reaches the limits of miniaturization. Because of its highly increased sensitivity, the quantum tunneling effect allows further miniaturization. This paper picks up this effect and presents a new design of a miniaturized accelerometer based on the tunneling effect. Figure 1 shows the principle of the sensor in a simplified way. The sensor consists of a spring mass system with several electrodes placed on the substrate. The two electrodes highlighted in red are used as electrostatic actuators for pulling down the tunneling tip to the operation point, controlling a constant distance between the tunneling electrodes and self-test actuations. The tunneling current depends exponentially on the distance  $d$  and is defined by

$$I_t = V_t \exp(-\alpha\sqrt{\Phi}d) \quad (1)$$

with the operational voltage of the tunnel sensor  $V_t$ , a constant  $\alpha_t = 1.024 \text{ eV}^{-0.5}\text{Å}^{-1}$ , the effective barrier height  $\Phi$ , and the distance  $d$  between the tunneling tips at the position where the tunneling current appears. The reasonable working distance between the tunneling electrodes is about 1 nm.

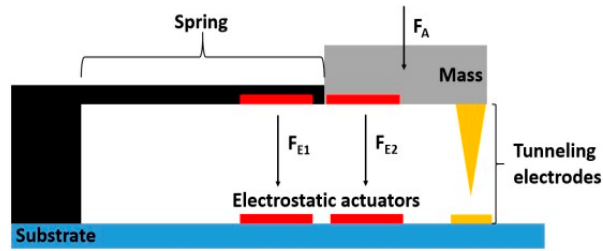


**Figure 1.** Principle of the tunneling accelerometer with its main components like the wafer substrate, the spring-mass-system, the electrostatic actuators and the tunneling section.

If an acceleration is applied to the system, the mass will be deflected and the tunneling current changes immediately. Due to the fact, that deflections in the range of sub-Angström already cause large changes in the tunneling current, a system of small size and consequently high stiffness can be designed.

Previous works have presented various highly accurate tunneling sensors developed in bulk micromechanics [1–5] as well as in surface micromachining [6–8]. For example, S. Patra shows a highaccuracy tunneling accelerometer with low rigidity and large-dimensioned mass to achieve resolutions in micro-g range [8]. C-H Liu [2] and T. Strobel [5] show tunneling sensors in bulk micromechanics with resolutions in a range of micro-g down to  $20 \text{ ng}/\sqrt{\text{Hz}}$ .

The aim of the present development is, largely independent of the resolution, the miniaturization up to the physical limits with a nominal acceleration of  $\pm 1 \text{ g}$ . The sensor structure is manufactured in surface micromachining by MEMSCAP Inc. (Durham, NC, USA). The platinum (Pt) tunneling electrode will be deposited subsequently to the sensor structure by a focused ion beam. The work of J. H. Daniel [9] presents a concept in which the tunneling section is created by separating a beam subsequently on a surface micromachining structure with a FIB.

## 2. Sensor Structure

The structure shown in Figure 2 resembles a helix shape and is designed in a way that the main displacement operates just in one direction. The model is the result of analytical and numerical calculations for high miniaturization with low first natural frequency for easy controllability that fulfils the design rules for manufacturing using PolyMUMPs process at MEMSCAP Inc. (Durham, NC, USA). The seismic mass (3) (PolySi) with a size ( $L \times W \times H$ ) of  $90 \mu\text{m} \times 85 \mu\text{m} \times 2 \mu\text{m}$  is suspended at the PolySi beam structure (2). The length of the beam (2) ( $W \times H$ :  $6 \mu\text{m} \times 1.5 \mu\text{m}$ ) from the anchor point (1) to the anchor of the mass (3) is  $405 \mu\text{m}$ . The PolySi pads (4) and (5) represent the supply lines for the electrostatic actuators.

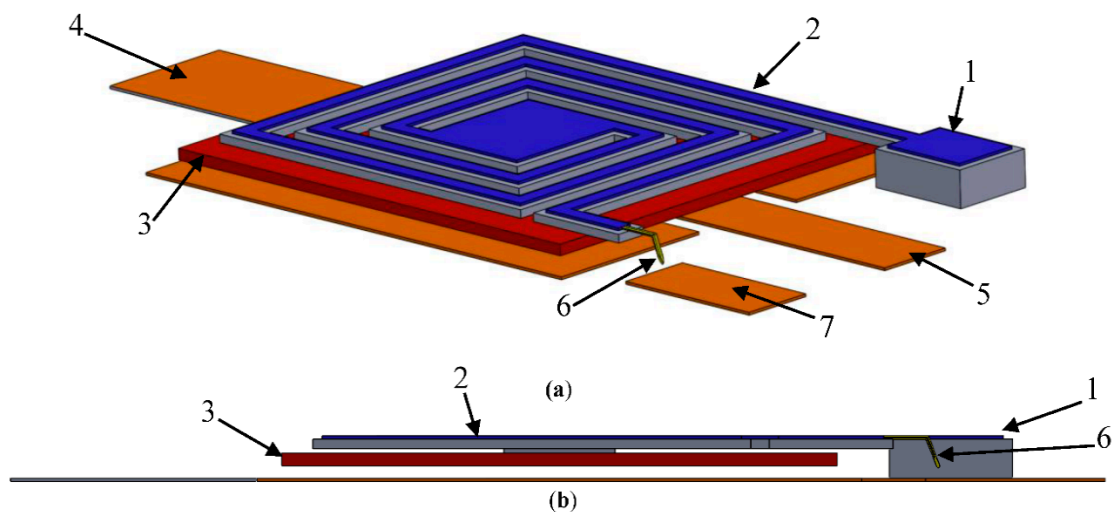


**Figure 2.** (a) Shows the 3D View of the CAD model of the sensor structure with anchor point (1), PolySi beam and metal layer (2), seismic mass (3), self-test pad (4), actuator pad (5), tunneling tip (6) and tunneling pad (7). (b) Shows the model in the side view.

(4) is used as a self-test actuator and (5) shows the actuator for the operating point and the control actuator. (6) points at the tunneling electrode (Pt) deposited to the sensor structure by a focused ion beam and (7) is the counter electrode of the tunneling tip. The force caused by the acting acceleration of 1 g results in a deflection of 9.36 Å. The first natural frequency of the structure amounts to 19 kHz.

### 3. Electrostatic Actuators

The electrostatic actuator is divided up into a stationary and a dynamic part. Figure 3a shows the positioning of the operation point actuator (5) which leads the sensor into operational conditions and keeps the voltage constant in the stationary mode. The electrostatic force

$$F_E = -\frac{1}{2} \epsilon_0 \epsilon_r \frac{A}{d} U_E^2 \quad (2)$$

is exerted by the electrostatic actuator with the dielectric constant  $\epsilon_0 = 8.85E - 12 \text{ As/V}$ , permittivity of air  $\epsilon_r = 1$ , area of the capacitor  $A$ , actuator voltage  $U_E$  and distance of the plates  $d$ . The area marked in grey shows the required deflection of the actuator in a range of between 40 and 80 nm or 9 and 12.5 V, depending on the starting distance of the tunneling electrodes due to the manufacturing tolerances of the FIB. Due to its preload and therefore high dynamics, this actuator is also used as control actuator. In order to compensate disturbances of +/-1 g at an operating voltage of  $U_{OP} = 11.1 \text{ V}$ , a differential voltage of just  $\Delta U = +/-80 \text{ mV}$  is required. Figure 3b shows the working range of the self-test actuator (4) for simulating a disturbance by voltage or electrostatic force. The example in Figure 3b illustrates a step of 1.8 V, corresponding to 0.5 g, which causes a deflection of 0.45 nm.

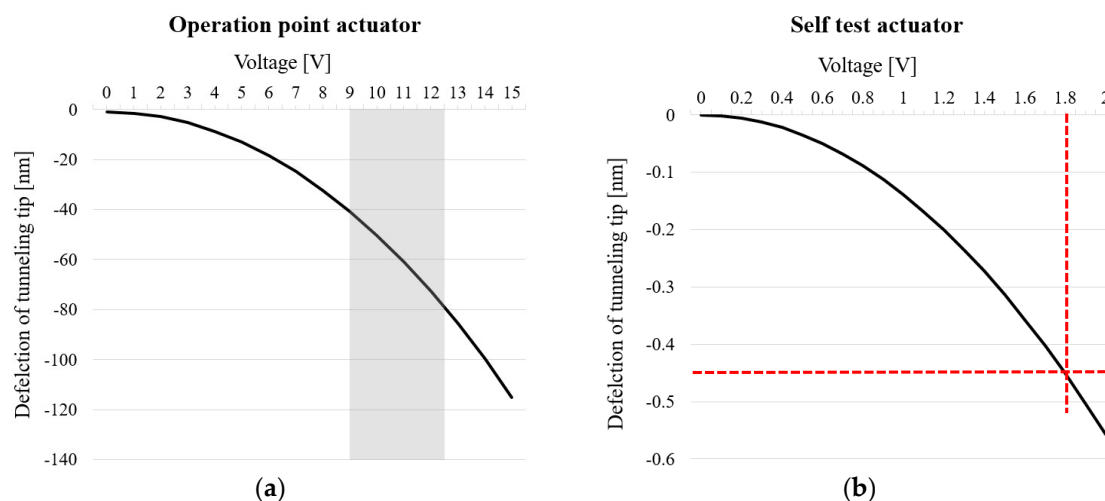


**Figure 3.** (a) Shows the deflection of the actuator reaching the operation point at 1 nm. Depending on the FIB deposition to manufacture the tunneling tip, the voltage varies between 9 and 12.5 V. The grey column shows the operation range. The impact of the self-test can be seen in (b). The example of a 0.5 g step is highlighted with dash lines.

### 4. Tunneling Tip

The manufacturing of the tunneling tips is performed by a focused ion beam. Ideally a tip of one platinum atom is provided, indeed we reach tips with diameters in a range of between 40 and 80 nm. The length of the tunneling section amounts to approximately 4 μm and runs from the gold layer at the endpoint of the structure to its counter electrode at the substrate, marked by (7) in Figure 2. After deposition and linking up the structure and the electrode the tunneling section is separated in two parts. Figure 4a shows exemplarily two connected beams deposited by the FIB with a minimum diameter of 65 nm. A cut of about 42 nm performed by the FIB is shown in (b). The resulting values of the cuts and beams are highly dependent on the chosen parameters. To ensure that the positions of the two tips do not shift after separation, low mechanical stress must be guaranteed.

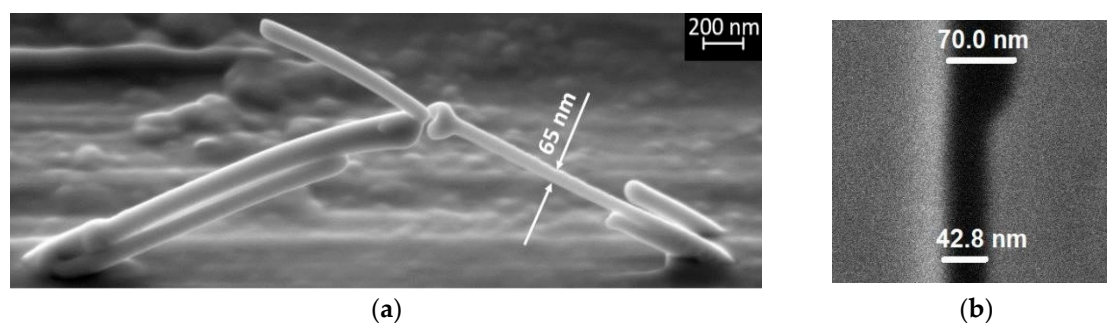


**Figure 4.** (a) Displays an example of two connected beams deposited by the focused ion beam with a minimum diameter of 65 nm; (b) illustrates a corresponding cut with a width in a range of between 42 and 70 nm at the substrate patterned by the FIB.

## 5. Conclusion and Summary

A further miniaturization of accelerometers requires a more sensitive principle than the capacitive, piezoresistive or piezoelectric effect. The tunneling effect enables the novel design of a miniaturized accelerometer presented in this paper with a small size of  $98 \times 85 \mu\text{m}^2$ . At an acting acceleration of 1 g the deflection of the tunneling tip is at  $9.36 \text{ \AA}$ . Two electrostatic actuators are implemented for controlling the deflection of the sensor structure. The main actuator pulls down the sensor structure until a tunneling current is measured and additionally acts as the control actuator after that due to its preload and high dynamics. The second actuator is used for simulating disturbances by providing an electrostatic force. The testing of the focused ion beam shows adequate results in deposition and patterning to realize the tunneling section.

**Acknowledgments:** This work is funded by the German Research Foundation (DFG).

**Conflicts of Interest:** The authors declare no conflict of interest.

## References

1. Rockstad, H.K.; Tang, T.K.; Reynolds, J.K.; Kenny, T.W.; Kaiser, W.J.; Gabrielson, T.B. A miniature, high-sensitivity, electron tunneling accelerometer. *Sens. Actuators A Phys.* **1996**, *53*, 227–231, doi:10.1016/0924-4247(96)01128-4.
2. Liu, C.-H.; Kenny, T.W. A High-Precision, Wide-Bandwidth Micromachined Tunneling Accelerometer. *J. Micromech. Syst.* **2001**, *10*, 425–433, doi:10.1109/84.946800.
3. Zavracky, P.M.; McClelland, B.; Warner, K.; Wang, J.; Hartley, F.; Dolgin, B. Design and process considerations for a tunneling tip accelerometer. *J. Micromech. Microeng.* **1996**, *6*, 352358, doi:10.1088/0960-1317/6/3/008.
4. Miao, M.; Hu, Q.; Hao, Y.; Dong, H.; Wang, L.; Shi, Y.; Shen, S. A bulk micromachined Si-on-glass tunneling accelerometer with out-of-plane sensing capability. In Proceedings of the IEEE International Conference on Nano/Micro Engineered and Molecular Systems, Bangkok, Thailand, 16–19 January 2007.
5. Strobelt, T. Hochauflösende Beschleunigungssensoren mit Tunnelstrecke. Ph.D. Thesis, University of Stuttgart, Stuttgart, Germany, 3 July 2000.
6. Kobayashi, D.; Hirano, T.; Furuhashi, T.; Fujita, H. An Integrated lateral tunneling unit. In Proceedings of the IEEE Micro Electro Mechanical Systems, Travemünde, Germany, 4–7 February 1992.
7. Kubena, R.L.; Atkinson, G.M.; Robinson, W.P.; Stratton, F.P. A new miniaturized surface micromachined tunneling accelerometer. *IEEE Electron Device Lett.* **1996**, *17*, 306–308, doi:10.1109/55.496466.
8. Patra, S.; Bhattacharyya, T.K. Design and Fabrication of micromachined tunneling accelerometers with micro-g resolution and their comparison. In Proceedings of the International Workshop on Electron Devices and Semiconductor Technology, Mumbai, India, 1–2 June 2009.
9. Daniel, J.H.; Moore, D.F. A microaccelerometer structure fabricated in silicon-on-insulator using a focused ion beam process. *Sens. Actuators A Phys.* **1999**, *73*, 201–209, doi:10.1016/S0924-4247(98)00237-4.

